Received: March 23, 2024 Revised: June 26, 2024 Accepted: June 26, 2024

https://doi.org/10.1016/j.neurom.2024.06.498

Tonic Stimulation of Dorsal Root Ganglion Results in Progressive Decline in Recruitment of Aα/β-Fibers in Rats

Jordyn E. Ting, PhD[1]; Charli Ann Hooper, MS[2]; Ashley N. Dalrymple, PhD[2,3,4]; Douglas J. Weber, PhD[2,5]

ABSTRACT

Objectives: In this study, we aimed to characterize the recruitment and maintenance of action potential firing in Aα/β-fibers generated during tonic dorsal root ganglion stimulation (DRGS) applied over a range of clinically relevant stimulation parameters.

Materials and Methods: We delivered electrical stimulation to the L5 dorsal root ganglion and recorded antidromic evoked compound action potentials (ECAPs) in the sciatic nerve during DRGS in Sprague Dawley rats. We measured charge thresholds to elicit ECAPs in Aα/β-fibers during DRGS applied at multiple pulse widths (50, 150, 300, 500 μs) and frequencies (5, 20, 50, 100 Hz). We measured the peak-to-peak amplitudes, latencies, and widths of ECAPs generated during 180 seconds of DRGS, and excitation threshold changes to investigate potential mechanisms of ECAP suppression.

Results: Tonic DRGS produced ECAPs in Aα/β-fibers at charge thresholds below the motor threshold. Increasing the pulse width of DRGS led to a significant increase in the charge required to elicit ECAPs in Aα/β-fibers, while varying DRGS frequency did not influence ECAP thresholds. Over the course of 180 seconds, ECAP peak-to-peak amplitude decreased progressively in a frequency-dependent manner, where 5- and 100-Hz DRGS resulted in 22% and 87% amplitude reductions, respectively, and ECAP latencies increased from baseline measurements during DRGS at 10, 20, 50, and 100 Hz. Regardless of DRGS frequency, ECAP amplitudes recovered within 120 seconds after turning DRGS off. We determined that ECAP suppression may be attributed to increasing excitation thresholds for individual fibers during DRGS. Following 180 seconds of DRGS, an average of 7.33% increase in stimulation amplitude was required to restore the ECAP to baseline amplitude.

Conclusions: DRGS produces a progressive and frequency-dependent reduction in ECAP amplitude that occurs within and above the frequency range used clinically to relieve pain. If DRGS-mediated analgesia relies on Aβ-fiber activation, then the frequency or duty cycle of stimulation should be set to the lowest effective level to maintain sufficient activation of Aβ-fibers.

Keywords: Chronic pain, dorsal root ganglion, electrical stimulation, neuromodulation, rats

INTRODUCTION

Dorsal root ganglion stimulation (DRGS) provides effective relief for patients with chronic pain stemming from complex regional pain syndrome[1–4] and causalgia,[1] as well as pain in the groin,[5] knee,[6,7] and distal extremities.[8–10] Despite its clinical success, the mechanisms of action underlying DRGS-mediated analgesia are still unknown, but several recent studies have investigated potential DRGS mechanisms through preclinical and computational models.[11–15]

One potential mechanism that has been a focus of recent studies is the low-pass filtering of pain signals at the T-junction of C-fibers in the dorsal root ganglion (DRG).[11,13,16–21] T-junction filtering is due, in part, to the pseudounipolar structure of afferent neurons, where the cell body is attached to the peripheral and central axons via the T-junction and stem axon.[17,18,22–24] Action potentials originating from the periphery must pass through the T-junction to reach the spinal cord, and likewise, action potentials originating in the soma or stem axon must pass through the T-junction before propagating through either the peripheral or central axons. T-junction filtering is thought to be an activity-dependent

Address correspondence to: Douglas J. Weber, PhD, Carnegie Mellon University, 5000 Forbes Ave, Pittsburgh, PA 15213, USA. Email: dougweber@cmu.edu

[1] Department of Bioengineering, University of Pittsburgh, Pittsburgh, PA, USA;
[2] Department of Mechanical Engineering, Carnegie Mellon University, Pittsburgh, PA, USA;
[3] Department of Biomedical Engineering, University of Utah, Salt Lake City, UT, USA;
[4] Department of Physical Medicine and Rehabilitation, University of Utah, Salt Lake City, UT, USA; and
[5] Neuroscience Institute, Carnegie Mellon University, Pittsburgh, PA, USA

For more information on author guidelines, an explanation of our peer review process, and conflict of interest informed consent policies, please see the journal's Guide for Authors.

Source(s) of financial support: This study was supported by the National Institutes of Health Helping to End Addiction Long-term (HEAL) Initiative grants RM1NS128775 and U18EB029251 to D.J.W. Partial support also was provided by National Institutes of Health (1R01NS121028).

phenomenon occurring when trains of action potentials excite the soma, causing electrotonic hyperpolarization of the soma, stem axon, and T-junction, potentially generated by somatic SK channels.[13,21]

Another potential mechanism for DRGS-mediated pain relief is gate control,[25] which also is hypothesized to mediate analgesia during spinal cord stimulation (SCS).[25–28] The gate control theory, in part, postulates that interneurons in the substantia gelatinosa of the dorsal horn regulate the transmission of peripheral signals from afferent fibers entering the spinal cord.[25] Briefly, recruitment of large-diameter afferent fibers excites inhibitory interneurons that block or gate the transmission of nociceptive signals from small-diameter afferent fibers to projection neurons that transmit nociceptive signals to the brain, thereby reducing pain. Additionally, the gate control theory states that the ascending dorsal column system acts as a central control trigger that activates selective pain processing mechanisms that regulate properties of gate control.[25]

Studies have demonstrated the potential involvement of both mechanisms. For example, several studies found that only Aα- and Aβ-fibers, which transmit proprioceptive and touch information, respectively, are activated by DRGS within the range of stimulation parameters used in the clinic.[12,29–31] While prior work from our group and others has demonstrated that DRGS preferentially induces activity in large-diameter, myelinated fibers as opposed to smaller and unmyelinated fibers,[12,29] few studies have investigated how Aα- and Aβ-fibers respond to tonic DRGS over a longer duration (ie, multiple minutes) and whether responses evoked by stimulation change over time. To our knowledge, there is a lack of studies thoroughly examining the effects of tonic DRGS on evoked compound action potentials (ECAPs) in Aα- and Aβ-fibers.

In this study, we compared charge thresholds required to elicit responses from Aα/β-fibers across multiple pulse widths and frequencies around the clinical parameter range, and measured ECAP responses to DRGS from the sciatic nerve during 180-second intervals of stimulation. We observed a progressive and frequency-dependent decline in ECAP amplitude over the 180-second interval of stimulation and a gradual recovery to initial amplitude following cessation of DRGS. Our study demonstrates that DRGS preferentially activates large-diameter afferent fibers, supporting gate control as a potential mechanism of DRGS-mediated pain relief. However, if DRGS-mediated analgesia relies on Aβ-fiber activation, even in part, then the frequency or duty cycle of stimulation should be set to the lowest effective level to maintain sufficient activation of Aβ-fibers during long-term DRGS.

MATERIALS AND METHODS

Experimental Model

We performed nonsurvival experiments in a total of 20 adult Sprague Dawley rats (11 female, nine male; >eight weeks old; 200–500 g; Charles River Laboratories, Wilmington, MA). All procedures were approved by the Institutional Animal Care and Use Committee of Carnegie Mellon University (Pittsburgh, PA). We induced anesthesia with isoflurane (inhalation, 4%–5%) and maintained anesthesia with isoflurane (inhalation, 1.5%–2.5%) for the duration of the experiment. We applied lubricant to the eyes and administered an intramuscular injection of glycopyrrolate (2.5 mL/kg) to reduce salivary, tracheobronchial, and pharyngeal secretions. We monitored respiratory rate, core temperature, and blink and withdrawal reflexes throughout the experiment. After the experiment concluded, the animal was euthanized with isoflurane overdose (inhalation, 5%).

Surgery

Following induction, we shaved the lumbar region of the back and the dorsal aspect of the hindlimb. To expose the caudal portion of the L5 DRG, we made an incision over the L4-L6 lamina and performed a partial laminectomy of the L5 vertebra. We placed a bipolar, cylindrical electrode lead (platinum/iridium, contact length = 0.76 mm, interelectrode spacing = 0.5 mm; Abbott Neuromodulation, Plano, TX) over the dorsal aspect of the L5 DRG to deliver DRGS.

We exposed the sciatic nerve ipsilateral to the target DRG and bluntly dissected the nerve from the surrounding muscle and connective tissue. We placed a tripolar cuff electrode (1.5-mm diameter; Micro-Leads, Somerville, MA) around the nerve to measure evoked responses. We also inserted a pair of intramuscular needle electrodes into the triceps surae muscle group for bipolar electromyography, and a ground electrode either between the skin and fascia of the hindlimb or near the base of the tail. After the experiment concluded, we measured the distance along the sciatic nerve from the stimulation site on the DRG to the recording site on the sciatic nerve (mean ± standard deviation, 50.0 ± 2.7 mm; $N = 20$ animals) to determine the conduction velocity (CV) of evoked responses in each animal.

Experimental Design and Analysis

We delivered bipolar electrical stimulation to the L5 DRG using symmetric, biphasic waveforms of varying current-amplitude, pulse width, and frequency, depending on the experimental paradigm (see *Recruitment*, *Tonic DRGS,* and *Mechanisms of ECAP Suppression*). While DRGS was delivered, we recorded ECAPs from the sciatic nerve cuff electrodes. Electroneurogram (ENG) signals were sampled from the sciatic nerve cuff electrode at 30 kHz and digitized using an Intan headstage and recording system (RHD2216, Intan Technologies, Los Angeles, CA) (Fig. 1a). We used conduction velocities to determine which afferent fiber types were contributing to each identified ECAP (Aα/β: >14 m/s; Aδ: 2.2–8 m/s; C: <1.2 m/s).[32] We calculated conduction velocities of the ECAPs using the distance between the DRGS and cuff electrodes and the latency of the first peak of the ECAP. We performed all processing and analysis of the data in MATLAB (MathWorks, Natick, MA). We bandpass-filtered (300–3000 Hz) the ENG data before further processing to identify ECAPs. We blanked stimulation artifacts over a time window ranging from 100 μs to 1 ms in duration, depending on the pulse width applied in a particular trial.

Recruitment

We conducted experiments to measure the charge threshold for recruiting Aα/β-fibers by DRGS. We varied stimulus pulse width and frequency around the typical clinical parameters (300 μs, 20 Hz)[1,13] to test the effects of varying each parameter on Aα/β-fiber activation thresholds (AT), or the charge required to elicit a detectable ECAP, and Aα/β-fiber recruitment. When testing for pulse width effects, we delivered DRGS at 20 Hz with pulse widths of 50, 150, 300, and 500 μs. When testing for frequency effects, we applied DRGS at frequencies of 5, 20, 50, and 100 Hz using 300-μs pulses. In each trial, we randomized the amplitude of DRGS current-pulses to generate recruitment curves of ECAPs recorded from the sciatic nerve. For each amplitude level, we applied 50 to 300 pulses

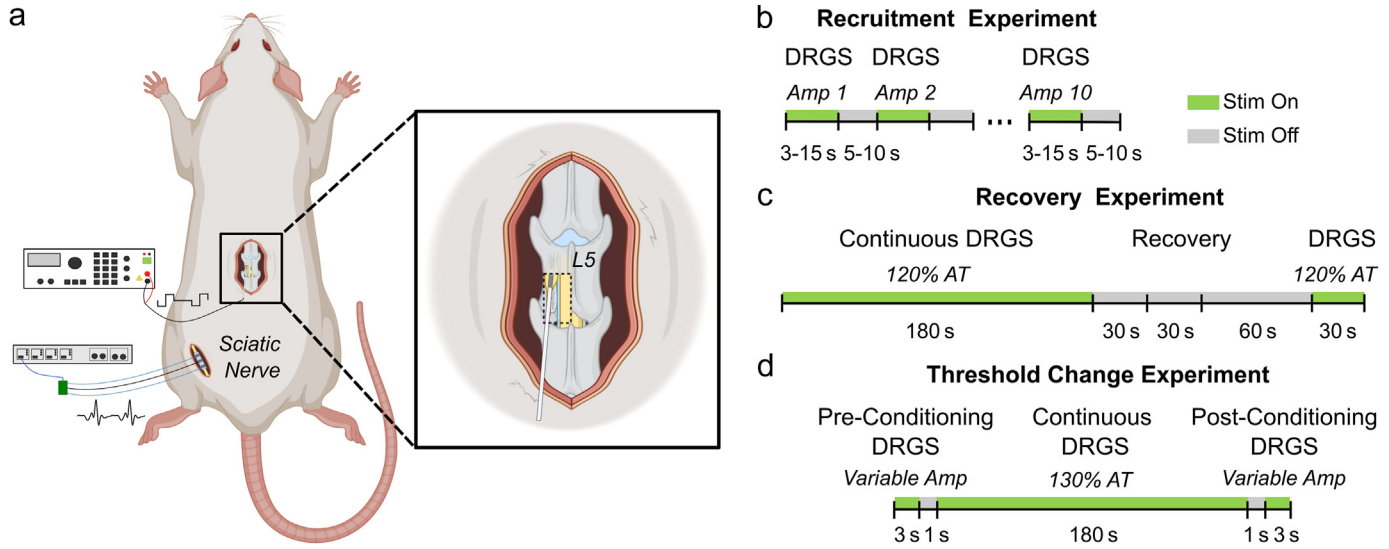

Figure 1. Experimental setup and stimulation protocols. a. In the DRGS experiments, a partial laminectomy was performed to expose the caudal portion of the L5 DRG, and a bipolar stimulation lead was placed over the DRG under the remaining bone. Neural activity was measured from a tripolar nerve cuff electrode placed around the sciatic nerve ipsilateral to the stimulation site. Stimulation protocols for the recruitment (panel b), recovery (panel c), and threshold change (panel d) experiments show the amplitude levels and durations of time that DRGS was on or off. AT, activation threshold (μA); Amp, amplitude (μA). [Color figure can be viewed at www.neuromodulationjournal.org]

(3–15 seconds) to the DRG with a 5- to 10-second interval between different amplitude levels. We also measured motor thresholds (MTs) for each pulse width and frequency parameter combination. We considered MT to be the charge level at which a muscle contraction was visible in the hindlimb.

For each DRGS current-amplitude level, we used a bootstrapping method, described in detail in prior studies[30,33], to detect Aα/β-fiber ECAPs. Briefly, stimulus-triggered averages (STA) were generated from random samples of the ENG recorded during 80% of the total stimulus repetitions (50–300). Depending on DRGS frequency, we produced 50 random STA samples for trials with 5-Hz DRGS and 100 samples for trials with 20-, 50-, or 100-Hz DRGS for each trial. The RMS of each averaged ENG signal was calculated using a 100-μs sliding window with 33-μs overlap with the previous window. The ECAP detection threshold was defined as one standard deviation greater than the upper bound of the 99% CI of the baseline RMS amplitude during a 1-millisecond period before each stimulus. An ECAP was successfully identified in a given trial if the same 100-μs RMS window contained suprathreshold values for 95% of the random samples. Automatically detected ECAPs were validated by visual inspection. We defined the Aα/β-fiber AT for a given recruitment trial as the lowest DRGS charge level (current-amplitude × pulse width; nC) with a detected ECAP.

To compare initial ECAP amplitudes elicited at AT, amplitudes from each tested frequency (5, 10, 20, 50, and 100 Hz) were averaged to yield one value per frequency for each animal. The mean amplitudes from each animal were normalized to the mean value at 20 Hz for the corresponding animal. The amplitudes from one animal were excluded because no 20-Hz trials were run during that experimental session that could be used for normalization.

Unless stated otherwise, numerical results are reported as mean ± standard deviation. We performed one-way analysis of variance (ANOVA) and Tukey–Kramer post-hoc tests with α-level of 0.05 to assess differences in ATs due to DRGS frequency or pulse width. We performed paired, two-tailed *t*-tests with α-level of 0.05 to compare Aα/β-fiber AT and MT in corresponding trials. We performed one-way ANOVA and Tukey–Kramer post-hoc tests with α-level of 0.05 to evaluate differences in initial ECAP amplitudes due to DRGS frequency.

Tonic DRGS

To study whether evoked responses changed during extended periods of stimulation and to assess the time necessary for ECAP amplitude to recover fully, we delivered DRGS continuously in 180-second intervals (Recovery Experiment) (Fig. 1c) at pulse frequencies of 5, 10, 20, 50, and 100 Hz. To determine the recovery time, we turned off DRGS for an interval of varying duration (30–120 seconds; recovery phase) before turning it on for an additional 30 seconds to measure ECAP amplitudes after the recovery phase. In all results shown, we used 300-μs pulses and a current amplitude equaling 120% of AT, which was determined for each tested frequency before conducting tonic DRGS experiments.

We measured ECAP amplitudes throughout each 180-s bout of tonic DRGS (Fig. 2). We identified ECAPs occurring during a time window corresponding to the latency of Aα/β-fiber responses. Specifically, we calculated the peak-to-peak amplitude of each ECAP elicited during 1-second windows immediately after the onset of DRGS (ie, 0–1 seconds after onset for 0 second time point) and at 1-second intervals throughout each 180-second trial. We normalized each ECAP measurement by subtracting the peak-to-peak of the baseline ENG activity (measured in a 0.5-millisecond window occurring before each DRGS pulse) from the peak-to-peak of the ECAP to account for any changes in the baseline noise level during trials. We calculated the mean and standard deviation of the ECAP amplitudes in each 1-second window and used these values for further processing. We averaged across amplitudes in 1-second windows in all trials, regardless of DRGS frequency, meaning that DRGS at 5 Hz resulted in five amplitude

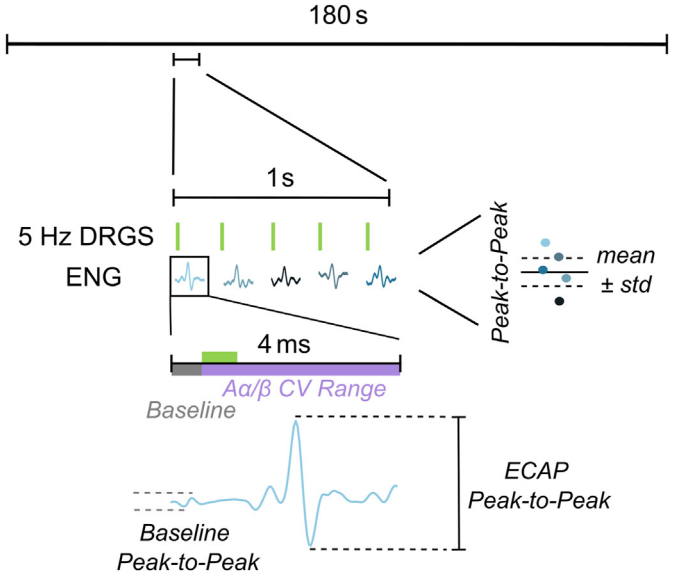

Figure 2. ECAP peak-to-peak measurement. ECAPs were identified from the 180-s ENG recording in 1-s windows. In each 1-s window, there were between five and 100 stimulus pulses, depending on DRGS frequency (5-Hz example shown above). We measured the peak-to-peak of the ENG within a window corresponding to the Aα/β-CV range (>14 m/s) and subtracted the peak-to-peak of the baseline ENG in a 0.5-ms window before the stimulus pulse to yield a single ECAP peak-to-peak measurement for each pulse. We repeated this process for each pulse and calculated the mean and standard deviation (std) of all peak-to-peak measurements within the 1-s window. [Color figure can be viewed at www.neuromodulationjournal.org]

measurements per 1-second interval, whereas DRGS at 100 Hz yielded 100 measurements.

Additionally, we fit the ECAP amplitude (A_{ECAP}) measurements obtained from each trial with exponential decay functions (ie, $A_{ECAP} = b_1 e^{b_2 t} + b_3$, where t is time during DRGS) and obtained the reported decay time constants (ie, b_2) from each fit. We excluded a small number of fits that were not statistically significant ($p > 0.05$) and fits in which the value of the decay constant fell outside of three standard deviations of the mean decay constant for that particular frequency group (3.7% of total fits excluded). We pooled the time constants across all trials and animals to yield a single mean value and standard deviation for each tested frequency (median adjusted $R^2 = 0.74$). We calculated the final ECAP amplitude for each trial as the mean of the last 15 seconds of amplitude measurements from the exponential fit. To measure the rate and extent of ECAP recovery, we compared the peak-to-peak amplitude measured in the first 1-second interval of DRGS after the variable-length recovery phase with the ECAP amplitude measured immediately after onset of the initial tonic DRGS period (ie, baseline level). We performed linear regression to model the recovery rate of ECAPs during the 180-second interval following cessation of tonic DRGS for each frequency group. A linear model of the form $y = mx + b$ was used, where x is the time in seconds since cessation of DRGS and y is the amplitude of the ECAP, measured as a percentage of the initial ECAP amplitude. The slope (m) in this model represents the recovery rate, and the intercept (b) represents the ECAP amplitude at the end of the 180-second period of tonic DRGS. We considered ECAP amplitude to be recovered fully when its difference from the baseline amplitude was not statistically significant.

We performed one-way ANOVA and Tukey–Kramer post-hoc tests with α-level of 0.05 to evaluate differences in decay constants, final ECAP amplitudes, and recovered ECAP amplitudes after 120 seconds due to DRGS frequency.

Mechanisms of ECAP Suppression

To explore potential mechanisms underlying the effects of tonic DRGS on Aα/β-fiber recruitment, we measured ECAP latency and width at baseline and at the time point corresponding to a 50% reduction in ECAP amplitude. ECAP latency and width may provide insight into the desynchronization of neuronal firing contributing to ECAP amplitude or changes in the conduction velocities across a subset of fibers.[34–36] Desynchronization of the fibers contributing to the ECAP may result in a lower response amplitude being measured during DRGS without the response being attenuated. In this case, a consistent population of fibers would be excited by stimulation but at slightly different times, resulting in a delayed and wider ECAP. ECAP latency and width measurements were obtained from the average ECAP trace in 1-second windows during DRGS. We defined the ECAP latency as the time from stimulus onset to the time of the positive peak of the ECAP identified within the Aα/β-CV window. To measure ECAP width, we identified both peaks of the ECAP and defined the start of the negative peak as the midpoint between the positive and negative peak amplitudes. We then determined the halfway point of the negative peak between the start of the peak and full negative peak amplitude and used this amplitude to calculate the width. We identified the point at which the ENG signal crossed this half-amplitude point (*intersect* function, MATLAB) and defined the ECAP width as the time difference between these two intersection points. ECAP peaks and intersection points used to calculate width were plotted and visually inspected. Traces that did not contain identifiable ENG intersection points were excluded from further analysis. Specifically, trials were excluded if fewer than ten ECAP measurements could be obtained from a 15-second window around the time point corresponding to a 50% reduction in amplitude (4.4% of total trials excluded). Lastly, we performed paired, two-tailed *t*-tests with α-level of 0.05 to compare ECAP latencies or ECAP widths at baseline and at 50% of ECAP amplitude.

We also performed experiments to determine whether fibers contributing to the ECAP were undergoing changes in their excitation thresholds during tonic DRGS. We delivered a preconditioning period (3 seconds) of DRGS, followed immediately (~1 second) by tonic DRGS for 180 seconds to evaluate ECAPs before and after tonic DRGS (Threshold Change Experiment) (Fig. 1d). Then, we applied DRGS during a postconditioning period (3 seconds) ~1 second after turning tonic DRGS off. ECAPs detected during the preconditioning period served as a baseline for comparing responses detected during the postconditioning period. Again, we delivered tonic DRGS at a range of frequencies (5, 20, 50, and 100 Hz) using 300-μs pulses and current amplitudes equaling 130% of AT. We delivered pre- and postconditioning periods of DRGS with the same frequency and pulse width as tonic DRGS; however, the current amplitudes for the pre- and postconditioning periods were incremented by 1 μA in each subsequent trial to determine the current level at which pre- and postconditioning ECAPs were approximately equal in size.

To compare ECAP amplitude in the Threshold Change Experiments (Fig. 1d), we generated an STA to yield a mean ECAP waveform for each of the 3-second pre- and postconditioning

phases of DRGS. We calculated the peak-to-peak amplitude from the mean ECAPs for the pre- and postconditioning phases of each trial. We then used these amplitudes to calculate the ratio of postconditioning ECAP amplitude to preconditioning ECAP amplitude as a percentage. If this value was ≥90%, the pre- and postconditioning ECAP amplitudes were considered to be approximately equal.

We performed a one-way ANOVA and Tukey–Kramer post-hoc test with α-level of 0.05 to evaluate differences in the current level required to generate an average ECAP in the postconditioning phase that was at least 90% of initial ECAP amplitude due to DRGS frequency. Additionally, we performed a paired *t*-test of both the ECAP latencies and ECAP widths, comparing the values measured during the pre- and postconditioning phases; values obtained across all frequencies were grouped.

RESULTS

ECAP Recruitment Thresholds

The AT for recruiting Aα/β-fibers was measured across a range of DRGS pulse widths and frequencies spanning the clinical parameter range. The average CV for ECAPs was 47.4 ± 7.0 m/s, which is within the CV range for Aα/β-fibers[32] ($N = 38$ trials/seven animals). ECAPs from Aδ- and C-fibers were not detected. The ATs to elicit ECAPs in Aα/β-fibers were significantly lower (54% ± 16%) than the MTs ($p < 0.001$; $N = 28$ trials/five animals) (Fig. 3c). The AT increased with stimulation pulse width (50 μs: 7.4 ± 2.2 nC; 150 μs: 9.2 ± 1.9 nC; 300 μs: 10.5 ± 3.4 nC; 500 μs: 15.5 ± 3.7 nC; $p < 0.001$; $N = 26$ trials/seven animals) (Fig. 3a). Specifically, increasing DRGS pulse width to 500 μs resulted in significantly larger ATs compared with all other pulse widths (50 vs 500 μs: $p < 0.001$; 150 vs 500 μs: $p < 0.01$; 300 vs 500 μs: $p < 0.05$). Varying DRGS frequency, however, between 5, 20, 50, and 100 Hz did not change the ATs required to excite Aα/β-fibers (5 Hz: 13.9 ± 3.8 nC; 20 Hz: 10.9 ± 4.3 nC; 50 Hz: 12.0 ± 3.2 nC; 100 Hz: 11.3 ± 3.1 nC; $p = 0.51$; $N = 38$ trials/ten animals) (Fig. 3b).

ECAP Amplitude Decline

ECAP peak-to-peak amplitudes at the onset of DRGS were compared across frequencies because lower stimulation frequencies have been shown to produce larger ECAPs in a previous study of SCS.[37] Mean initial ECAP amplitudes were 2.23 times larger when DRGS was delivered at 5 Hz (the lowest tested frequency) compared with DRGS delivered at the typical clinical frequency of 20 Hz, and significantly different from DRGS at 10, 50, and 100 Hz ($p < 0.001$; 10 Hz: 1.35, 5 Hz vs 10 Hz: $p < 0.05$; 20 Hz: 1, 5 Hz vs 20 Hz: $p < 0.001$; 50 Hz: 1.16, 5 Hz vs 50 Hz: $p < 0.01$; 100 Hz: 1.05, 5 Hz vs 100 Hz: $p < 0.001$; $N = 10$ animals) (Fig. 3d).

While DRGS frequency did not affect the charge level required to elicit an ECAP in Aα/β-fibers, frequency did have an effect on the maintenance of ECAP amplitude during extended intervals of DRGS, as shown in representative examples from trials across frequencies (Fig. 4). ECAPs remained clearly distinguishable from background

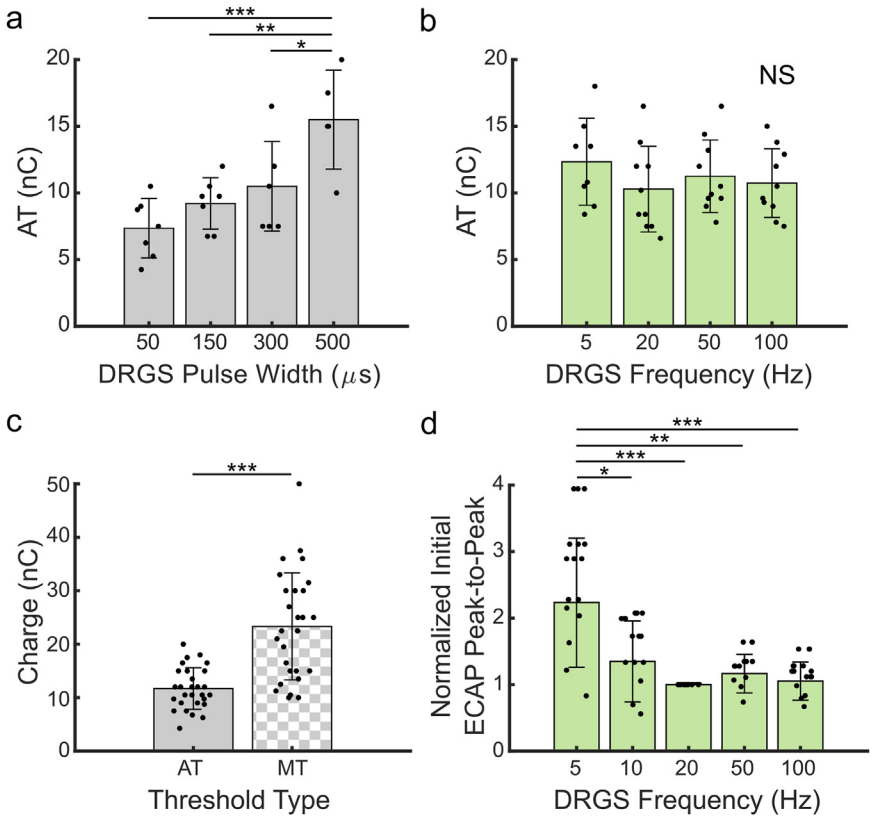

Figure 3. DRGS sensory and motor thresholds. a. ATs were measured from the sciatic nerve during DRGS with varying pulse widths and (panel b) frequencies. c. MTs were measured from the triceps surae muscle and compared with activation thresholds across all stimulation parameters. d. ECAP peak-to-peak amplitudes were measured during the first 1 s after DRGS onset and normalized to the 20-Hz condition from the same animal for comparing amplitudes across frequencies. *$p < 0.05$; **$p < 0.01$; ***$p < 0.001$. nC, nanocoulomb. [Color figure can be viewed at www.neuromodulationjournal.org]

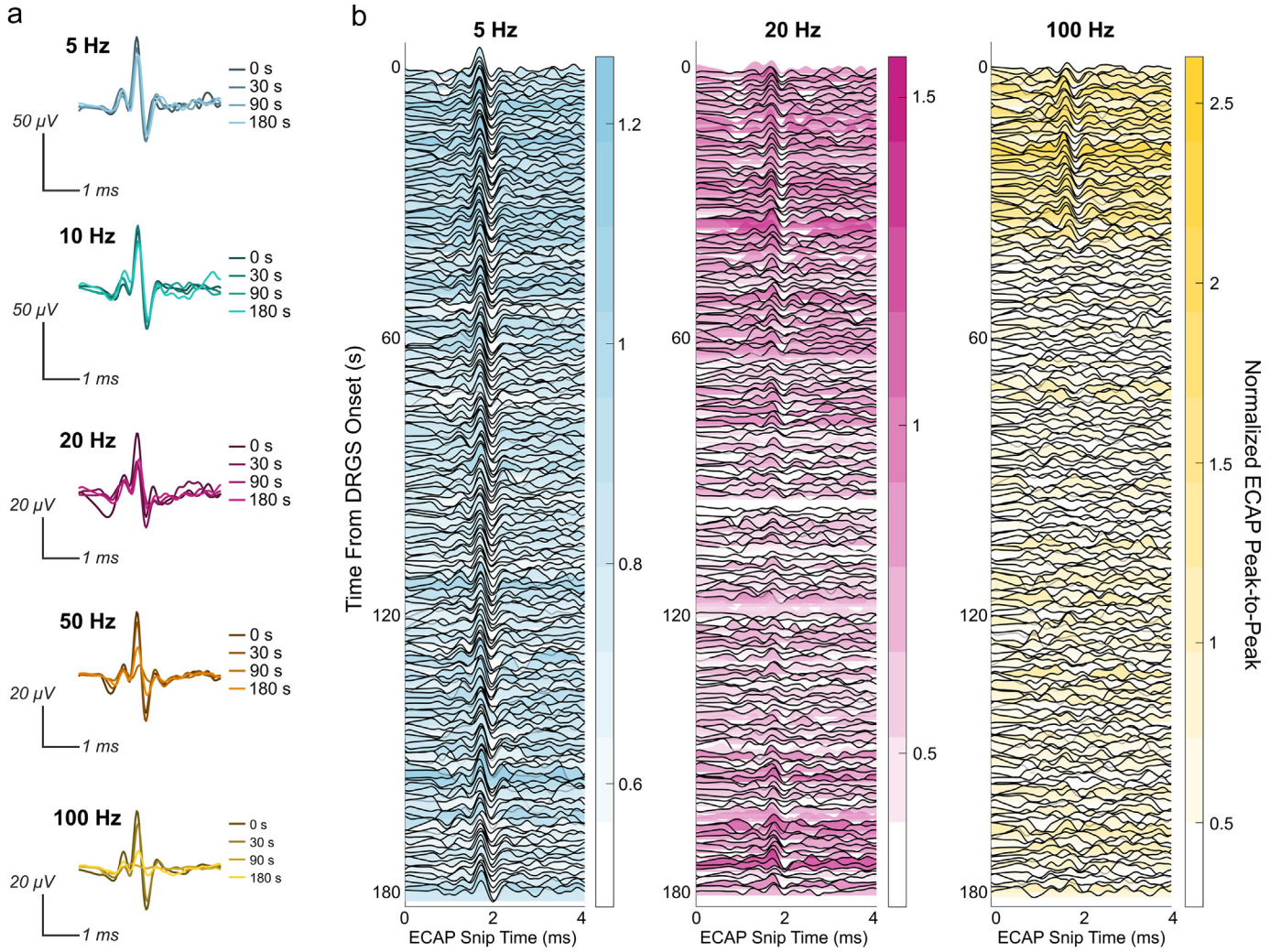

Figure 4. ECAP amplitude reduction during tonic DRGS. Example ECAPs recorded in five separate trials during a single experimental session are shown. ECAP waveform peak-to-peak amplitude declines progressively from onset (0 s) throughout the course of 180-s tonic DRGS delivered at 5, 10, 20, 50, and 100 Hz. a. Each ECAP waveform represents the average waveform over a 1-s interval at 0, 30, 90, or 180 s after onset of DRGS. b. Average ECAP waveforms from the same example trials (5, 20, and 100 Hz) are shown at intervals of 1 s throughout the full 180-s stimulation period. Stimulus pulses were delivered at 0 s, and the artifact was blanked during postprocessing. [Color figure can be viewed at www.neuromodulationjournal.org]

noise during 5- and 10-Hz DRGS, while ECAPs diminished much more noticeably during 20-, 50-, and 100-Hz DRGS (Fig. 4a). ECAPs generated during 5-Hz DRGS exhibited only a slight decrease in amplitude (Fig. 4b). During 20-Hz DRGS, ECAP size was reduced during the first 60 to 90 seconds of stimulation and returned with a diminished amplitude for the final 30 seconds of the trial (Fig. 4b). When DRGS was delivered at 100 Hz, ECAPs experienced a sharp reduction in amplitude, making them indistinguishable from baseline noise after approximately 30 seconds (Fig. 4b).

ECAP amplitudes declined progressively during the 3-minute course of stimulation across DRGS frequencies from 5 to 100 Hz. This progressive decline in ECAP amplitude was fitted by an exponential decay function for each frequency of DRGS (Fig. 5a). After 180 s of tonic DRGS, ECAP amplitudes decreased from baseline levels (measured 0-1 second after DRGS onset) in a frequency-dependent manner to 77.9% ± 25.7% of initial size at 5 Hz and 13.1% ± 8.0% at 100 Hz (10 Hz: 57.0% ± 12.8%; 20 Hz: 33.9% ± 11.6%; 50 Hz: 28.1% ± 12.8%; $p < 0.001$) (Fig. 5b). DRGS delivered at 50 Hz did not produce significantly different reductions compared with DRGS at 20 Hz ($p = 0.73$); however, all other frequency pairs were significantly different ($p < 0.019$). Increasing DRGS frequency also significantly increased the magnitude of the decay constant of the corresponding exponential functions ($p < 0.001$), leading to a quicker loss of ECAP amplitude when DRGS was delivered at higher rates (5 vs 20 Hz: $p < 0.05$; 5 vs 50 Hz: $p < 0.001$; 5 vs 100 Hz: $p < 0.001$; 10 vs 50 Hz: $p < 0.001$; 10 vs 100 Hz: $p < 0.001$; 20 vs 50 Hz: $p < 0.05$; 20 vs 100 Hz: $p < 0.001$) (Fig. 5c).

ECAP Recovery

We paused stimulation for 120 seconds to study the recovery of ECAP amplitude following each 180-second period of tonic DRGS. ECAPs were measured at 0, 30, 60, and 120 seconds following cessation of DRGS. Across all conditions, ECAP amplitudes returned to baseline during the 120-second recovery period ($p > 0.05$) (Fig. 6b). When DRGS was delivered at 5 Hz, however, ECAP amplitudes returned to baseline within 60 seconds of DRGS

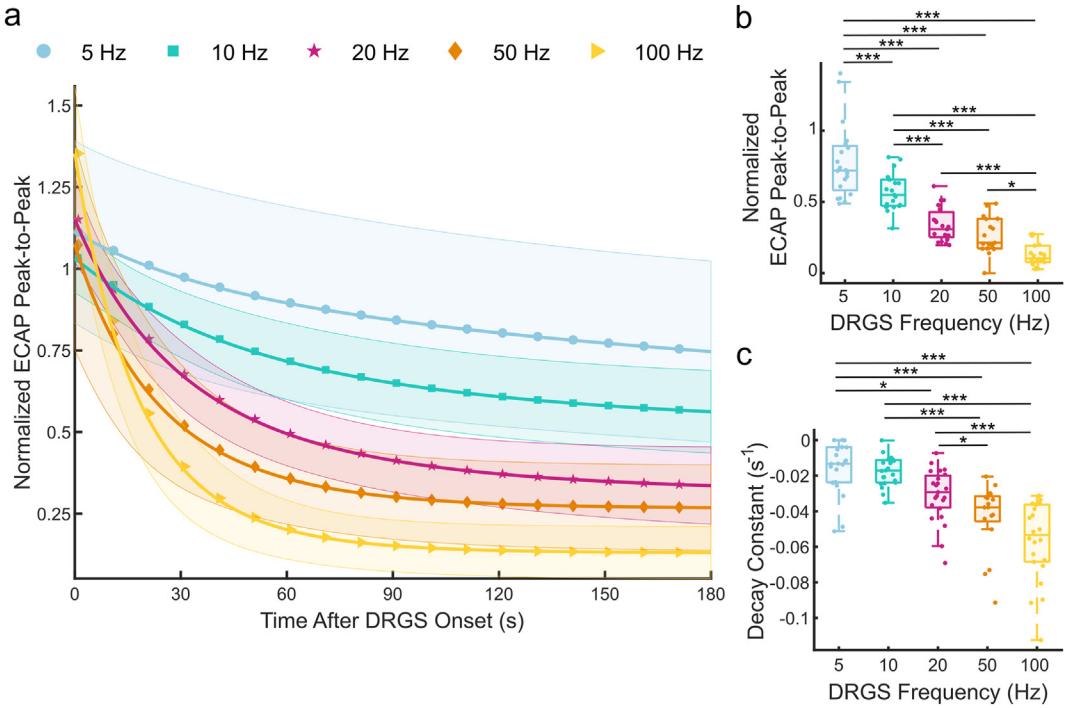

Figure 5. Frequency-dependent exponential decline in ECAP amplitude. a. Normalized ECAP peak-to-peak amplitudes calculated at 1-s intervals during tonic DRGS were fit with one-term exponential functions. The mean of the fitted values across all trials and standard deviation are shown. b. The mean normalized ECAP peak-to-peak amplitude over the final 15 s of tonic DRGS and (panel c) the decay constant for each fit are shown. *$p < 0.05$; ***$p < 0.001$. [Color figure can be viewed at www.neuromodulationjournal.org]

cessation. We approximated the rate of recovery as the slope of the linear fit to the average ECAP amplitude vs recovery time, from 0 to 120 seconds (Fig. 6b). The rates of recovery, expressed as changes in normalized ECAP amplitude per second, ranged from 0.22% following 5-Hz DRGS to 0.65% following 50-Hz DRGS.

Potential Mechanisms of ECAP Decline

To determine whether desynchronization may be causing the reduction in Aα/β-ECAP amplitude, we measured ECAP latency and width. We compared mean ECAP latencies (or widths) recorded during the first 15 s following DRGS onset (0–15 seconds) with mean latencies (or widths) during a 15-second interval immediately after the ECAP amplitudes were diminished by 50% from baseline in all Recovery Experiment trials. We determined this second time point using the exponential fits for each tonic DRGS trial (Fig. 5a). ECAP latencies increased significantly from the onset of DRGS to the time point at which ECAP amplitudes were diminished to 50% of baseline size during DRGS delivered at 20 ($p < 0.01$), 50 ($p < 0.001$), and 100 Hz ($p < 0.001$) (Fig. 7b). Overall, ECAP latencies also increased during 10-Hz DRGS, but the change was not statistically significant ($p = 0.106$). Mean ECAP latency increases were 0.052 ± 0.079 milliseconds at 10 Hz, 0.025 ± 0.031 milliseconds at 20 Hz, 0.051 ± 0.033 milliseconds at 50 Hz, and 0.067 ± 0.055 milliseconds at 100 Hz (Fig. 7b,c). ECAP peak width did not change significantly from the onset of DRGS to the time point at which ECAP peak-to-peak amplitudes were reduced to 50% of baseline size across all frequencies ($p > 0.05$) (Fig. 7d).

We sought to determine whether tonic DRGS could increase the excitation thresholds for eliciting Aα/β-ECAPs by varying the amplitude of the DRGS current-amplitude delivered (N = seven animals). We hypothesized that tonic DRGS led to an increase in the excitation thresholds of a subset of Aα/β-fibers contributing to the ECAP. To measure these changes, we delivered DRGS for a period of 3 seconds at a fixed current-amplitude (preconditioning), followed by 180 seconds of tonic DRGS at 130% AT, and finally, a second period of DRGS for 3 seconds at the initial current-amplitude (postconditioning) (Fig. 1d). We compared the peak-to-peak amplitudes of the mean ECAP waveforms during the pre- and postconditioning periods of DRGS. After conditioning with 180 seconds of tonic DRGS, the ECAP size was reduced but could be recovered fully (ie, ≥90% initial ECAP amplitude) by increasing the amplitude of the DRGS pulse by an average of 7.33% over the amplitude used during the conditioning interval (130% AT) (Fig. 8). DRGS frequency did not have a significant effect on the current level required to recover the ECAP amplitude to initial size ($p = 0.754$). However, the mean increase in current required did trend higher as DRGS frequency increased (Fig. 8b). The latencies of the ECAPs that recovered to at least 90% of their initial amplitude were significantly slower in the postconditioning phase (1.444 ± 0.099 milliseconds) than in the preconditioning phase (1.422 ± 0.102 milliseconds) of the corresponding trial ($p < 0.001$). The widths of the recovered responses did not change between the pre- (0.171 ± 0.028 milliseconds) and postconditioning (0.165 ± 0.021 milliseconds) phases ($p > 0.05$).

DISCUSSION

In this study, we examined the effects of tonic DRGS applied over a range of frequencies on antidromic, evoked activity in Aα/β-fibers

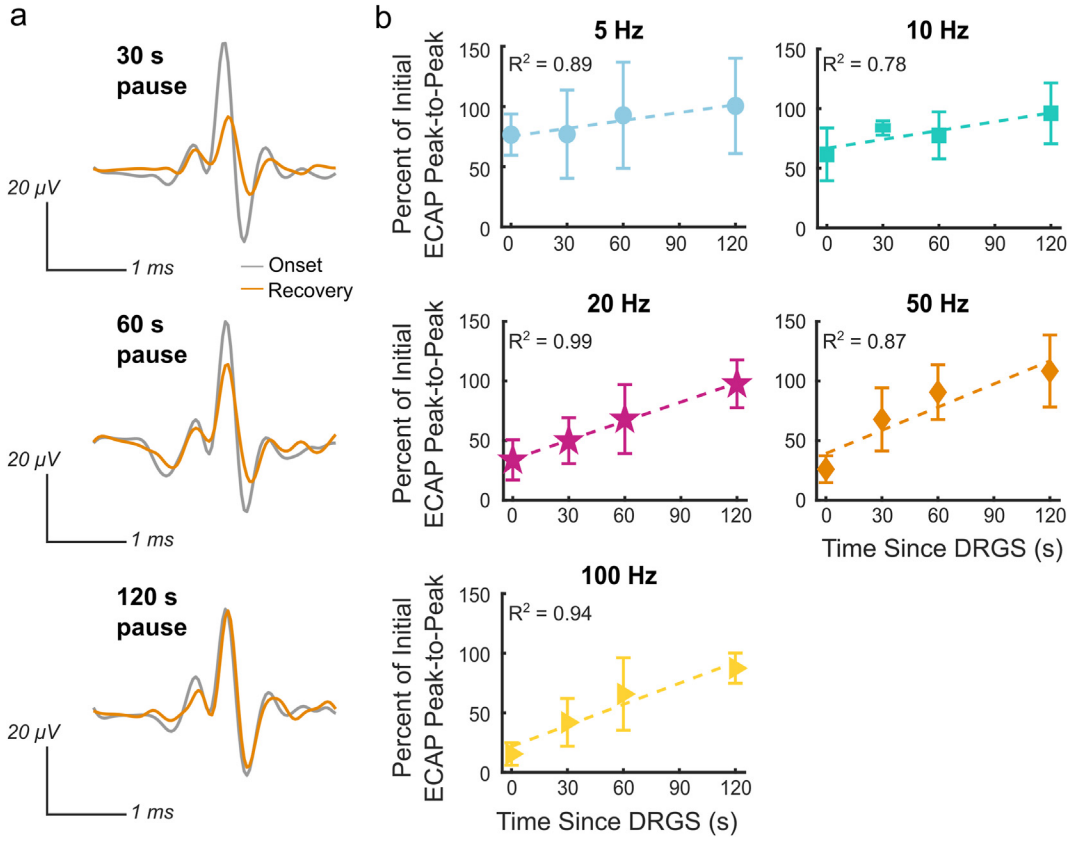

Figure 6. ECAP recovery following 180-s DRGS. a. Example ECAP waveforms recorded in three separate 50-Hz DRGS trials during a single experimental session are shown. Each panel shows the ECAP at onset of the tonic DRGS period (gray) and ECAP recorded immediately (0–1 s) following the recovery period (orange) of 30, 60, or 120 s (DRGS off). b. ECAP peak-to-peak amplitudes (mean ± standard deviation as percentage of initial ECAP amplitude) and corresponding linear fits of the average ECAP amplitudes are shown at 0 s since DRGS (end of tonic stimulation period) and recovery periods of 30, 60, and 120 s. The adjusted R^2 values are included for each fit. [Color figure can be viewed at www.neuromodulationjournal.org]

of the sciatic nerve. We first verified that DRGS recruits large-diameter afferent fibers, with conduction velocities consistent with Aα/β-fibers, at lower charge thresholds than are required to elicit hindlimb motor activity. We then stimulated the L5 DRG tonically for 180 seconds and showed a progressive, frequency-dependent reduction in the amplitude of peripheral ECAPs during stimulation that was subsequently recovered 120 seconds after discontinuing stimulation. Decreases in ECAP amplitude occurred during DRGS delivered at frequencies as low as 5 Hz, with the greatest reductions occurring during DRGS at 100 Hz. We also found that ECAP latencies increased significantly during DRGS delivered at 20 Hz or higher. However, ECAP widths were consistent throughout the stimulation period, demonstrating that the reduction in ECAP amplitude was unlikely due to desynchronization of firing in individual fibers contributing to the ECAP. Finally, we tested whether excitation threshold changes in individual fibers may be responsible for ECAP attenuation, and demonstrated that immediate and full recovery of the ECAP amplitude could be achieved by increasing the amplitude of DRGS pulses. Collectively, these results suggest that if DRGS-mediated analgesia relies on Aβ-fiber activation, then the frequency of stimulation should be set to the lowest possible level to maintain sufficient activation of Aβ-fibers. Alternatively, pausing DRGS periodically may allow recovery of Aβ-fiber excitability, sustaining their influence during tonic stimulation.

Recruitment Thresholds

In our recruitment experiments, we measured ATs for Aα/β-fiber ECAPs that were approximately 50% of the MT, which is consistent with our prior results in a feline model of DRGS.[29] We observed an expected relationship between stimulus pulse width and AT based on known charge-duration curves,[38,39] where increasing pulse width in a range from 50 to 500 μs resulted in an increase in the charge necessary to generate an ECAP in Aα/β-fibers.

We also verified that ATs were independent of stimulation frequency, within a range from 5 to 100 Hz. The relationship between stimulation frequency and recruitment is less well-defined than that of pulse width and recruitment, and prior studies have shown that higher frequencies of stimulation may lead to reduced ECAP amplitudes over extended periods of stimulation.[37,40] As hypothesized, we did not observe a significant effect of DRGS frequency on ATs required to elicit ECAPs in Aα/β-fibers. However, we did find that the peak-to-peak amplitude of the initial ECAPs recruited (ie, 0–1 second after DRGS onset) during DRGS at 120% AT intensity was significantly larger during 5-Hz stimulation than stimulation at higher frequencies.

ECAP Suppression

While DRGS effectively relieves chronic pain in the clinic, its mechanisms are not well understood. Few studies have

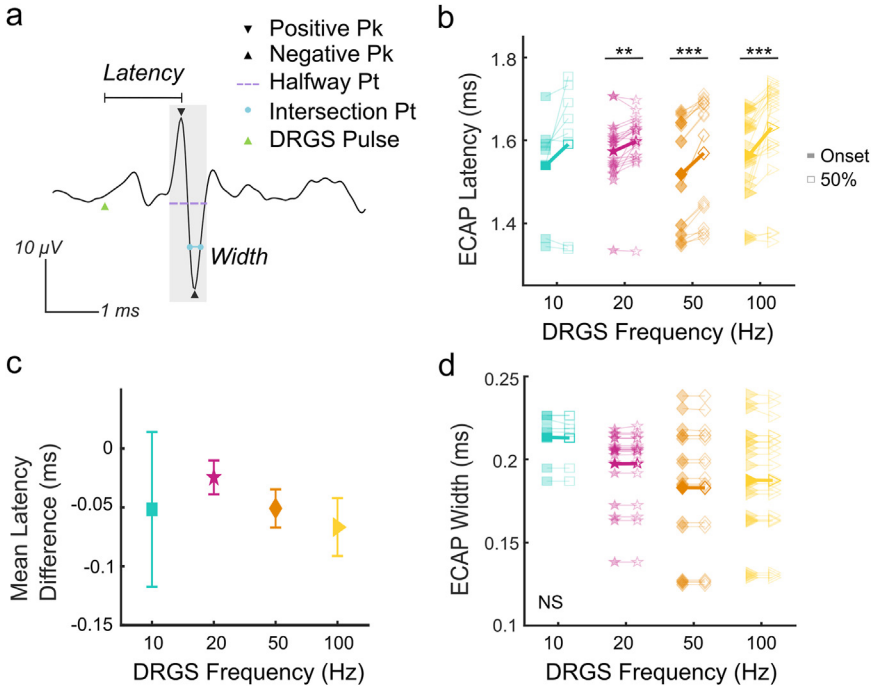

Figure 7. ECAP latency and width during DRGS. ECAP latency and width during DRGS. a. ECAP latency was defined as the time elapsed between the onset of the DRGS pulse and the positive peak of the ECAP waveform. ECAP width was measured from the intersection points midway between the halfway point (purple line) and the negative peak location. b. ECAP latencies measured at the onset of continuous DRGS were lower than the ECAP latencies measured at the time point in which ECAP peak-to-peak amplitudes were reduced to 50% of baseline size across frequencies. c. The mean differences in latency ranged from 25 (20 Hz) to 67 μs (100 Hz). Error bars represent 95% confidence bounds. d. ECAP width did not change significantly during DRGS across all frequencies. $^{**}p < 0.01$; $^{***}p < 0.001$. Pk, peak; Pt, point. [Color figure can be viewed at www.neuromodulationjournal.org]

investigated how afferent fibers respond to tonic DRGS,[11–13,16] and to our knowledge, there is a lack of studies examining how the recruitment of Aα/β-fibers changes during tonic DRGS. Herein, we observed a frequency-dependent reduction in peak-to-peak ECAP amplitude during tonic DRGS delivered at multiple frequencies between 5 and 100 Hz. We selected this particular frequency range to examine the effects of tonic DRGS on evoked activity because it is typically delivered clinically at frequencies between 20 and 40 Hz.[1,13] The depressive effect on ECAP amplitude was much greater at higher frequencies, resulting in a nearly complete suppression (87%) during 100-Hz stimulation. Although DRGS applied within this clinical frequency range did not produce complete

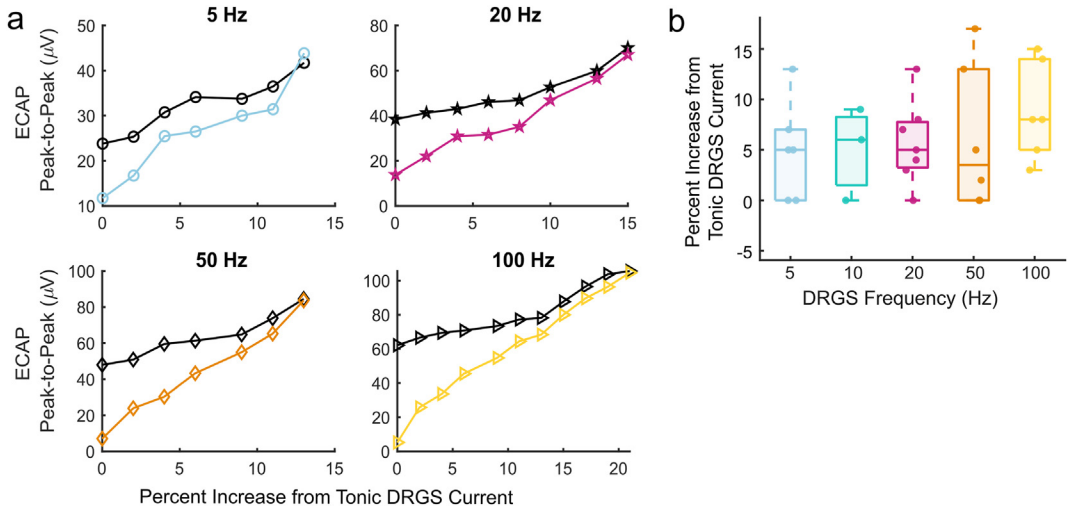

Figure 8. Threshold increases after tonic DRGS. a. The peak-to-peak amplitude of the average ECAPs recorded during the 3-s pre- (black line) and postconditioning DRGS intervals was calculated for each increasing current step from 130% AT for DRGS trials at 5, 20, 50, and 100 Hz as examples. b. The percentage increase from tonic DRGS current required to restore the ECAP to at least 90% of preconditioning ECAP amplitude in the postconditioning phase. [Color figure can be viewed at www.neuromodulationjournal.org]

suppression, stimulation at 20 and 50 Hz resulted in a 66% and 73% reduction in average ECAP amplitude, respectively. At lower frequencies, the ECAP attenuation during tonic DRGS was much lower; 5- and 10-Hz stimulation produced only 22% and 43% attenuation, respectively.

A similar reduction in ECAP amplitude has also been reported during SCS with electrodes positioned over the dorsal columns[37,40,41] in animal and human studies. A recent study in patients with SCS implants reported that increasing stimulation frequency from 2 to 455 Hz during conventional SCS resulted in progressively smaller ECAPs.[37] The authors suggested two potential explanations for the reduced ECAP size with increasing SCS frequency: increases in excitation thresholds[42–46] or intermittent conduction block[47–49] among a set of fibers. However, they were unable to investigate further because of their study design. Additionally, Shechter et al[40] showed that both conventional (50 Hz) and high-frequency (1 kHz) SCS delivered at a current intensity just below the Aδ-fiber excitation threshold decreased Aα/β-fiber ECAPs in the sciatic nerve induced by dorsal root stimulation in rats. However, SCS at a lower current-amplitude (ie, Aα/β-fiber excitation threshold) produced a reduction in ECAP amplitude only when stimulation was delivered at 1 kHz. In light of our findings, which were obtained using a much lower DRGS frequency range (5–100 Hz vs 1 kHz), these results may suggest that different mechanisms contribute to ECAP amplitude reduction during conventional SCS (40–60 Hz) or DRGS (20–40 Hz) and high-frequency stimulation paradigms.

Potential Mechanisms of ECAP Suppression

Recent studies have demonstrated that high-frequency SCS (1–10 kHz) excites Aα/β axons in the dorsal columns but in an asynchronous manner, where axons do not fire in response to every stimulus of a high-frequency pulse train.[41,47] Deep brain stimulation (DBS) studies have described a similar effect, in which axons were unable to respond reliably to pulse trains of higher frequencies (ie, 100 or 200 Hz), resulting in a frequency-dependent reduction in amplitude over the course of stimulation applied to the hippocampus[34,50] and subthalamic nucleus.[51] In comparison with stimulation frequencies reported in the SCS and DBS literature, we observed a reduction in ECAP amplitudes over a lower range of frequencies (5–100 Hz). Therefore, our findings are unlikely to result from the desynchronization of firing across fibers contributing to ECAPs.

An alternative explanation for ECAP attenuation during prolonged stimulation may involve changes in neuronal excitability that lead to increased excitation thresholds. Several studies have demonstrated that human cutaneous afferent fibers undergo activity-dependent decreases in excitability due to a hyperpolarization produced by electrogenic sodium/potassium pumps.[42,52–54] These increases in fiber threshold have been observed during sustained repetitive stimulation with frequencies as low as 8 Hz in humans but are larger with stimulation at higher frequencies of 20 and 30 Hz.[42] Furthermore, our results suggest that excitation threshold changes are likely a contributing factor to the observed ECAP decline. Herein, we demonstrated that an ECAP of equal size to baseline measurements could be obtained immediately following a 180-second bout of tonic DRGS with an increase in DRGS current amplitude of ~7% (Fig. 8). We also observed a trend, although not significant, indicating that higher DRGS frequencies produced greater decreases in excitability.

Clinical Significance

DRGS has been shown to be effective in relieving pain over a range of stimulation frequencies in both animal and clinical studies, although the mechanisms responsible for analgesia may depend on frequency. Achieving pain relief through low-frequency DRGS, specifically, is advantageous because it allows implanted stimulators to maintain longer battery life. Clinical studies have shown that DRGS with frequencies as low as 4 Hz is effective in maintaining pain relief in patients with chronic pain stemming from a variety of pain etiologies when DRGS frequency is tapered from initial levels of 16[55] or 20 Hz.[56] Stimulation delivered with frequencies at or under 5 Hz has been shown to inhibit pain through activation of low-threshold mechanoreceptors (LTMR), but LTMR activation hardly affects pain behavior when stimulation is applied with higher frequencies.[57] Koetsier et al[58] also reported no significant differences in the maximal pain-relieving effects of DRGS delivered at frequencies of 1, 20, and 1000 Hz in rats with painful diabetic polyneuropathy. DRGS applied only at 1 Hz resulted in a delayed washout effect, leading the authors to suggest that 1-Hz DRGS specifically may stimulate Aδ-fibers and induce Aδ-mediated long-term depression in the dorsal horn.[58,59] We did not observe Aδ-fiber activation with the DRGS current-amplitude levels and frequencies (≥5 Hz) used in our study; however, we did likely activate Aβ-LTMRs with our stimulation parameters. In the present study, we observed much less suppression of Aα/β-ECAP responses during 5-Hz DRGS as compared with higher frequencies. Taken together with studies highlighting the clinical effectiveness of low-frequency DRGS, our results suggest that maintaining more consistent Aα/β-fiber activation during tonic DRGS may be important for achieving pain relief.

We observed a progressive (ie, time-dependent) and frequency-dependent decline in Aα/β-fiber recruitment during tonic DRGS that resulted in at least a 50% reduction for stimulation frequencies at or above 20 Hz. Gate-control mechanisms may still be partially effective when nearly 50% of Aα/β-fibers remain activated. However, with the large reduction in Aα/β recruitment at increasing frequencies, DRGS may be less likely to engage gate-control mechanisms to produce long-term analgesia at these frequencies.[25] Alternative mechanisms for DRGS-mediated analgesia include T-junction filtering and local γ-aminobutyric acid (GABA)-mediated gating. T-junction filtering results in a decreased rate of action potentials passing through the central axon during repeated stimulation.[11,13,16–21] This filtering effect has been shown to occur primarily in C- and Aδ-fibers during DRGS delivered at frequencies between 5 and 100 Hz.[11] However, it has also been shown to affect Aβ-fibers, but to a much smaller degree and primarily during DRGS delivered at higher frequencies (ie, 50 and 100 Hz).[11] Filtering of painful signals transmitted through C- and Aδ-fibers has been shown to play a role in analgesia, but the DRGS AT for type C neurons has been reported to be ~1.5 times higher than the AT for type A neurons.[11]

Nociceptive signaling may also be attenuated through GABA-mediated gating occurring within the DRG itself.[60] Notably, DRGS has been shown to not cause an increase in extracellular GABA within the dorsal horn.[61] Du et al[60] (2017), however, showed that depolarizing stimuli cause a release of GABA from large-, medium-, and small-diameter DRG neurons and that an infusion of GABA or GABA reuptake inhibitors into the DRG relieves neuropathic pain. Therefore, excitation of large-diameter fibers, as we have shown in the present study, may lead to GABA-mediated gating that, in turn, results in decreased signaling through small-diameter fibers and a reduction in pain.

The neuronal mechanisms of pain have been shown to differ between females and males;[62,63] however, clinical studies of DRGS and SCS show similar pain relief in both female and male participants.[64–66] While we did not design our study to address differences in DRGS recruitment due to sex, we performed a post-hoc analysis to evaluate the effects of sex on ECAP attenuation. After grouping the data across frequencies, we found that ECAP attenuation was significantly stronger in female rats than in male rats (Supplementary Fig. 1). Additionally, ECAP attenuation was also significantly stronger in smaller rats (<306 grams) than in larger rats (>324 grams) included in this study (Supplementary Fig. 2).

Limitations

We performed our study in healthy, anesthetized animals because our primary aim was to characterize the effects of DRGS on large-diameter fiber recruitment. Without measuring ECAPs during DRGS in a pain model, it is unclear how the suppression of Aα/β-ECAPs contributes to pain perception. Therefore, future studies should examine how changes in Aα/β-ECAP amplitude contribute to changes in pain behavior during DRGS. Additionally, we chose to focus on DRGS frequency effects and, accordingly, stimulated at two current-amplitude levels proportional to AT (120% and 130% AT). Previous studies have defined an acceptable amplitude range to be <80% MT[11,67] in animal studies involving DRGS. Stimulation at 60% MT has been demonstrated to be effective in reflex behavioral testing, whereas DRGS at 80% MT has been shown to be effective in both reflex behavioral testing and conditioned place preference testing.[67] In clinical settings, DRGS is delivered at current levels capable of activating afferent fibers and generating paresthesias without inducing pain or muscle activity.[3,68–70] Therefore, we used AT as a metric for determining current levels and found that 120% AT or 130% AT were within an acceptable amplitude range to mimic clinical stimulation intensities.

Because we used nerve cuff electrodes for recording from the sciatic nerve, we were unable to detect single-unit activity from individual fibers within the nerve. Recording single-unit activity would allow us to measure changes in excitability of individual fibers and, therefore, confirm whether their excitation thresholds are indeed changing over the course of stimulation. It is also typically difficult to detect activity in small-diameter fibers, such as C-fibers, from antidromic ECAPs recorded from outside of the neural sheath and during electrical stimulation at frequencies greater than 1 Hz because of the activity-dependent slowing of successive action potentials.[71–74] In this study, however, our primary aim was to measure recruitment of Aα/β-fibers, which can be detected reliably from nerve cuff electrodes during stimulation delivered at all frequencies and with charge thresholds well below those shown to activate C-fibers.[11]

Additionally, we characterized antidromic responses in the peripheral nerve; however, signals entering the spinal cord through central axonal processes mediate the sensations perceived during electrical stimulation or pain. Peripheral ECAPs should be representative of firing occurring in the DRG and being propagated to the spinal cord, but signals propagating centrally may undergo additional filtering between the T-junction and central axonal process due to the smaller diameter of the central axon relative to the peripheral process.[17,18,21,24] However, the impedance mismatch primarily responsible for the low-pass filtering effect is due to the pseudounipolar structure of the primary sensory neuron.[17,18,21] Therefore, it is important to further investigate the effects of DRGS on Aα/β-neuron activity in the dorsal root or spinal cord to understand the central effects on pain.

CONCLUSIONS

In this study, we demonstrated that tonic DRGS recruits Aα/β-fibers with typical clinical stimulation parameters and generates a frequency-dependent reduction in the resulting ECAPs. ECAPs were diminished during DRGS applied at frequencies ranging from 5 to 100 Hz, with the greatest reductions occurring during higher stimulation frequencies. The observed suppression in ECAP amplitude may be attributed to increases in excitation thresholds of individual fibers contributing to the evoked response. Our findings provide further evidence that DRGS evokes activity in large-diameter afferent fibers, supporting gating in the dorsal horn as a potential mechanism of DRGS-mediated pain relief, although this evoked activity progressively decreases over extended periods of stimulation. However, if DRGS-mediated analgesia relies on Aβ-fiber activation, then the frequency or duty cycle of stimulation should be set to the lowest effective level to maintain sufficient activation of Aβ-fibers during long-term DRGS.

Acknowledgements

The authors thank Sharon John, Kestrel Merritt, and Sebastian Correa for their assistance during surgical procedures; Angela Malaney and the rodent facility staff at Carnegie Mellon University for their animal care services; and Ameya Nanivadekar from Abbott Neuromodulation for donating the electrodes.

Authorship Statements

Jordyn E. Ting and Douglas J. Weber designed the study. Jordyn E. Ting, Charli Ann Hooper, and Ashley N. Dalrymple collected the data. Jordyn E. Ting and Charli Ann Hooper analyzed the data. Jordyn E. Ting wrote the manuscript with input from Charli Ann Hooper, Ashley N. Dalrymple, and Douglas J. Weber. All authors edited and approved the manuscript.

Conflict of Interest

Jordyn E. Ting, Charli Ann Hooper, and Ashley N. Dalrymple report no conflicts of interest. Douglas J. Weber is a cofounder and shareholder of Reach Neuro, Inc., a consultant and shareholder of Neuronoff, Inc., a shareholder and scientific board member for NeuroOne Medical, Inc., and a cofounder and shareholder of Bionic Power, Inc.

How to Cite This Article

Ting J.E., Hooper C.A., Dalrymple A.N., Weber D.J. 2024. Tonic Stimulation of Dorsal Root Ganglion Results in Progressive Decline in Recruitment of Aα/β-Fibers in Rats. Neuromodulation 2024; ■: 1–13.

SUPPLEMENTARY DATA

To access the supplementary material accompanying this article, visit the online version of *Neuromodulation: Technology at the Neural Interface* at www.neuromodulationjournal.org and at https://doi.org/10.1016/j.neurom.2024.06.498.

REFERENCES

1. Deer TR, Levy RM, Kramer J, et al. Dorsal root ganglion stimulation yielded higher treatment success rate for complex regional pain syndrome and causalgia at 3 and 12 months: a randomized comparative trial. *Pain*. 2017;158:669–681. https://doi.org/10.1097/j.pain.0000000000000814.
2. Liem L, Russo M, Huygen FJPM, et al. One-year outcomes of spinal cord stimulation of the dorsal root ganglion in the treatment of chronic neuropathic pain. *Neuromodulation*. 2015;18:41–48 [discussion: 48]. https://doi.org/10.1111/ner.12228.
3. Van Buyten J-P, Smet I, Liem L, Russo M, Huygen F. Stimulation of dorsal root ganglia for the management of complex regional pain syndrome: a prospective case series. *Pain Pract*. 2015;15:208–216. https://doi.org/10.1111/papr.12170.
4. Yang A, Hunter CW. Dorsal root ganglion stimulation as a salvage treatment for complex regional pain syndrome refractory to dorsal column spinal cord stimulation: a case series. *Neuromodulation*. 2017;20:703–707. https://doi.org/10.1111/ner.12622.
5. Liem L, Mekhail N. Management of postherniorrhaphy chronic neuropathic groin pain: a role for dorsal root ganglion stimulation. *Pain Pract*. 2016;16:915–923. https://doi.org/10.1111/papr.12424.
6. van Bussel CM, Stronks DL, Huygen FJPM. Dorsal column stimulation vs. dorsal root ganglion stimulation for complex regional pain syndrome confined to the knee: patients' preference following the trial period. *Pain Pract*. 2018;18:87–93. https://doi.org/10.1111/papr.12573.
7. van Bussel CM, Stronks DL, Huygen FJPM. Successful treatment of intractable complex regional pain syndrome type I of the knee with dorsal root ganglion stimulation: a case report. *Neuromodulation*. 2015;18:58–60 [discussion: 60]. https://doi.org/10.1111/ner.12190.
8. Kretzschmar M, Reining M, Schwarz MA. Three-year outcomes after dorsal root ganglion stimulation in the treatment of neuropathic pain after peripheral nerve injury of upper and lower extremities. *Neuromodulation*. 2021;24:700–707. https://doi.org/10.1111/ner.13222.
9. Chapman KB, Van Roosendaal B-KW, Van Helmond N, Yousef TA. Unilateral dorsal root ganglion stimulation lead placement with resolution of bilateral lower extremity symptoms in diabetic peripheral neuropathy. *Cureus*. 2020;12:e10735. https://doi.org/10.7759/cureus.10735.
10. Garg A, Danesh H. Neuromodulation of the cervical dorsal root ganglion for upper extremity complex regional pain syndrome-case report. *Neuromodulation*. 2015;18:765–768. https://doi.org/10.1111/ner.12307.
11. Chao D, Zhang Z, Mecca CM, Hogan QH, Pan B. Analgesic dorsal root ganglionic field stimulation blocks conduction of afferent impulse trains selectively in nociceptive sensory afferents. *Pain*. 2020;161:2872–2886. https://doi.org/10.1097/j.pain.0000000000001982.
12. Graham RD, Bruns TM, Duan B, Lempka SF. Dorsal root ganglion stimulation for chronic pain modulates Aβ-fiber activity but not C-fiber activity: a computational modeling study. *Clin Neurophysiol*. 2019;130:941–951. https://doi.org/10.1016/j.clinph.2019.02.016.
13. Kent AR, Min X, Hogan QH, Kramer JM. Mechanisms of dorsal root ganglion stimulation in pain suppression: a computational modeling analysis. *Neuromodulation*. 2018;21:234–246. https://doi.org/10.1111/ner.12754.
14. Graham RD, Jhand AS, Lempka SF. Dorsal root ganglion stimulation produces differential effects on action potential propagation across a population of biophysically distinct C-neurons. *Front Pain Res (Lausanne)*. 2022;3:1017344. https://doi.org/10.3389/fpain.2022.1017344.
15. Koetsier E, Franken G, Debets J, et al. Effectiveness of dorsal root ganglion stimulation and dorsal column spinal cord stimulation in a model of experimental painful diabetic polyneuropathy. *CNS Neurosci Ther*. 2019;25:367–374. https://doi.org/10.1111/cns.13065.
16. Chao D, Mecca CM, Yu G, et al. Dorsal root ganglion stimulation of injured sensory neurons in rats rapidly eliminates their spontaneous activity and relieves spontaneous pain. *Pain*. 2021;162:2917–2932. https://doi.org/10.1097/j.pain.0000000000002284.
17. Gemes G, Koopmeiners A, Rigaud M, et al. Failure of action potential propagation in sensory neurons: mechanisms and loss of afferent filtering in C-type units after painful nerve injury. *J Physiol*. 2013;591:1111–1131. https://doi.org/10.1113/jphysiol.2012.242750.
18. Du X, Hao H, Gigout S, et al. Control of somatic membrane potential in nociceptive neurons and its implications for peripheral nociceptive transmission. *Pain*. 2014;155:2306–2322. https://doi.org/10.1016/j.pain.2014.08.025.
19. Gemes G, Rigaud M, Koopmeiners AS, Poroli MJ, Zoga V, Hogan QH. Calcium signaling in intact dorsal root ganglia: new observations and the effect of injury. *Anesthesiology*. 2010;113:134–146. https://doi.org/10.1097/ALN.0b013e3181e0ef3f.
20. Koopmeiners AS, Mueller S, Kramer J, Hogan QH. Effect of electrical field stimulation on dorsal root ganglion neuronal function. *Neuromodulation*. 2013;16:304–311 [discussion: 310]. https://doi.org/10.1111/ner.12028.
21. Sundt D, Gamper N, Jaffe DB. Spike propagation through the dorsal root ganglia in an unmyelinated sensory neuron: a modeling study. *J Neurophysiol*. 2015;114:3140–3153. https://doi.org/10.1152/jn.00226.2015.
22. Stoney SD. Limitations on impulse conduction at the branch point of afferent axons in frog dorsal root ganglion. *Exp Brain Res*. 1990;80:512–524. https://doi.org/10.1007/BF00227992.
23. Lüscher C, Streit J, Lipp P, Lüscher HR. Action potential propagation through embryonic dorsal root ganglion cells in culture. II. Decrease of conduction reliability during repetitive stimulation. *J Neurophysiol*. 1994;72:634–643. https://doi.org/10.1152/jn.1994.72.2.634.
24. Lüscher C, Streit J, Quadroni R, Lüscher HR. Action potential propagation through embryonic dorsal root ganglion cells in culture. I. Influence of the cell morphology on propagation properties. *J Neurophysiol*. 1994;72:622–633. https://doi.org/10.1152/jn.1994.72.2.622.
25. Melzack R, Wall PD. Pain mechanisms: a new theory. *Science*. 1965;150:971–979. https://doi.org/10.1126/science.150.3699.971.
26. Sufka KJ, Price DD. Gate control theory reconsidered. *Brain Mind*. 2002;3:277–290. https://doi.org/10.1023/A:1019996809849.
27. Wall PD, Sweet WH. Temporary abolition of pain in man. *Science*. 1967;155:108–109. https://doi.org/10.1126/science.155.3758.108.
28. Shealy CN, Mortimer JT, Reswick JB. Electrical inhibition of pain by stimulation of the dorsal columns: preliminary clinical report. *Anesth Analg*. 1967;46:489–491.
29. Dalrymple AN, Ting JE, Bose R, et al. Stimulation of the dorsal root ganglion using an Injectrode. *J Neural Eng*. 2021;18:056068. https://doi.org/10.1088/1741-2552/ac2ffb.
30. Nanivadekar AC, Ayers CA, Gaunt RA, Weber DJ, Fisher LE. Selectivity of afferent microstimulation at the DRG using epineural and penetrating electrode arrays. *J Neural Eng*. 2019;17:016011. https://doi.org/10.1088/1741-2552/ab4a24.
31. Graham RD, Bruns TM, Duan B, Lempka SF. The effect of clinically controllable factors on neural activation during dorsal root ganglion stimulation. *Neuromodulation*. 2021;24:655–671.
32. Harper AA, Lawson SN. Conduction velocity is related to morphological cell type in rat dorsal root ganglion neurones. *J Physiol*. 1985;359:31–46. https://doi.org/10.1113/jphysiol.1985.sp015573.
33. Ayers CA, Fisher LE, Gaunt RA, Weber DJ. Microstimulation of the lumbar DRG recruits primary afferent neurons in localized regions of lower limb. *J Neurophysiol*. 2016;116:51–60. https://doi.org/10.1152/jn.00961.2015.
34. Jensen AL, Durand DM. High frequency stimulation can block axonal conduction. *Exp Neurol*. 2009;220:57–70. https://doi.org/10.1016/j.expneurol.2009.07.023.
35. Bhadra N, Kilgore KL. Direct current electrical conduction block of peripheral nerve. *IEEE Trans Neural Syst Rehabil Eng*. 2004;12:313–324. https://doi.org/10.1109/TNSRE.2004.834205.
36. Casey KL, Blick M. Observations on anodal polarization of cutaneous nerve. *Brain Res*. 1969;13:155–167. https://doi.org/10.1016/0006-8993(69)90150-4.
37. Gmel GE, Santos Escapa R, Parker JL, Mugan D, Al-Kaisy A, Palmisani S. The effect of spinal cord stimulation frequency on the neural response and perceived sensation in patients with chronic pain. *Front Neurosci*. 2021;15, 625835.
38. Merrill DR, Bikson M, Jefferys JGR. Electrical stimulation of excitable tissue: design of efficacious and safe protocols. *J Neurosci Methods*. 2005;141:171–198. https://doi.org/10.1016/j.jneumeth.2004.10.020.
39. Durand DM. Electrical stimulation of excitable systems. In: *The Biomedical Engineering Handbook*. Taylor & Francis; 2006:474–495.
40. Shechter R, Yang F, Xu Q, et al. Conventional and kilohertz-frequency spinal cord stimulation produces intensity- and frequency-dependent inhibition of mechanical hypersensitivity in a rat model of neuropathic pain. *Anesthesiology*. 2013;119:422–432. https://doi.org/10.1097/ALN.0b013e31829bd9e2.
41. Sagalajev B, Zhang T, Abdollahi N, et al. Paresthesia during spinal cord stimulation depends on synchrony of dorsal column axon activation. bioRxiv. https://doi.org/10.1101/2023.01.10.523167
42. Kiernan MC, Lin CSY, Burke D. Differences in activity-dependent hyperpolarization in human sensory and motor axons. *J Physiol*. 2004;558:341–349. https://doi.org/10.1113/jphysiol.2004.063966.
43. Gasser HS. Changes in nerve-potentials produced by rapidly repeated stimuli and their relation to the responsiveness of nerve to stimulation. *American Journal of Physiology-Legacy Content*. 1935;111:35–50. https://doi.org/10.1152/ajplegacy.1935.111.1.35.
44. Bostock H, Grafe P. Activity-dependent excitability changes in normal and demyelinated rat spinal root axons. *J Physiol*. 1985;365:239–257. https://doi.org/10.1113/jphysiol.1985.sp015769.
45. Jansen JKS, Nicholls JG. Conductance changes, an electrogenic pump and the hyperpolarization of leech neurones following impulses. *J Physiol*. 1973;229:635–655. https://doi.org/10.1113/jphysiol.1973.sp010158.
46. Morita K, David G, Barrett JN, Barrett EF. Posttetanic hyperpolarization produced by electrogenic Na(+)-K+ pump in lizard axons impaled near their motor terminals. *J Neurophysiol*. 1993;70:1874–1884. https://doi.org/10.1152/jn.1993.70.5.1874.
47. Crosby ND, Janik JJ, Grill WM. Modulation of activity and conduction in single dorsal column axons by kilohertz-frequency spinal cord stimulation. *J Neurophysiol*. 2017;117:136–147. https://doi.org/10.1152/jn.00701.2016.

48. Guo Z, Feng Z, Wang Y, Wei X. Simulation study of intermittent axonal block and desynchronization effect induced by high-frequency stimulation of electrical pulses. *Front Neurosci*. 2018;12:858. https://doi.org/10.3389/fnins.2018.00858.
49. Bellinger SC, Miyazawa G, Steinmetz PN. Submyelin potassium accumulation may functionally block subsets of local axons during deep brain stimulation: a modeling study. *J Neural Eng*. 2008;5:263–274. https://doi.org/10.1088/1741-2560/5/3/001.
50. Feng Z, Wang Z, Guo Z, Zhou W, Cai Z, Durand DM. High frequency stimulation of afferent fibers generates asynchronous firing in the downstream neurons in hippocampus through partial block of axonal conduction. *Brain Res*. 2017;1661:67–78. https://doi.org/10.1016/j.brainres.2017.02.008.
51. Zheng F, Lammert K, Nixdorf-Bergweiler BE, Steigerwald F, Volkmann J, Alzheimer C. Axonal failure during high frequency stimulation of rat subthalamic nucleus. *J Physiol*. 2011;589:2781–2793. https://doi.org/10.1113/jphysiol.2011.205807.
52. Applegate C, Burke D. Changes in excitability of human cutaneous afferents following prolonged high-frequency stimulation. *Brain*. 1989;112:147–164. https://doi.org/10.1093/brain/112.1.147.
53. Kiernan MC, Mogyoros I, Hales JP, Gracies JM, Burke D. Excitability changes in human cutaneous afferents induced by prolonged repetitive axonal activity. *J Physiol*. 1997;500:255–264. https://doi.org/10.1113/jphysiol.1997.sp022015.
54. Kiernan MC, Hales JP, Gracies JM, Mogyoros I, Burke D. Paraesthesiae Induced by Prolonged high frequency stimulation of human cutaneous afferents. *J Physiol*. 1997;501:461–471. https://doi.org/10.1111/j.1469-7793.1997.461bn.x.
55. Chapman KB, Yousef TA, Vissers KC, van Helmond N, Stanton-Hicks MD. Very low frequencies maintain pain relief from dorsal root ganglion stimulation: an evaluation of dorsal root ganglion neurostimulation frequency tapering. *Neuromodulation: Technology at the Neural Interface*. 2021;24:746–752. https://doi.org/10.1111/ner.13322.
56. Piedade GS, Gillner S, McPhillips PS, Vesper J, Slotty PJ. Effect of low-frequency dorsal root ganglion stimulation in the treatment of chronic pain. *Acta Neurochir*. 2023;165:947–952. https://doi.org/10.1007/s00701-023-05500-1.
57. Arcourt A, Gorham L, Dhandapani R, et al. Touch receptor-derived sensory information alleviates acute pain signaling and fine-tunes nociceptive reflex coordination. *Neuron*. 2017;93:179–193. https://doi.org/10.1016/j.neuron.2016.11.027.
58. Koetsier E, Franken G, Debets J, et al. Dorsal root ganglion stimulation in experimental painful diabetic polyneuropathy: delayed wash-out of pain relief after low-frequency (1Hz) stimulation. *Neuromodulation*. 2020;23:177–184. https://doi.org/10.1111/ner.13048.
59. Sandkühler J, Chen JG, Cheng G, Randić M. Low-frequency stimulation of afferent Aδ-fibers induces long-term depression at primary afferent synapses with substantia gelatinosa neurons in the rat. *J Neurosci*. 1997;17:6483–6491. https://doi.org/10.1523/JNEUROSCI.17-16-06483.1997.
60. Du X, Hao H, Yang Y, et al. Local GABAergic signaling within sensory ganglia controls peripheral nociceptive transmission. *J Clin Invest*. 2017;127:1741–1756. https://doi.org/10.1172/JCI86812.
61. Koetsier E, Franken G, Debets J, et al. Mechanism of dorsal root ganglion stimulation for pain relief in painful diabetic polyneuropathy is not dependent on GABA release in the dorsal horn of the spinal cord. *CNS Neurosci Ther*. 2020;26:136–143. https://doi.org/10.1111/cns.13192.
62. Dedek A, Xu J, Lorenzo L-É, et al. Sexual dimorphism in a neuronal mechanism of spinal hyperexcitability across rodent and human models of pathological pain. *Brain*. 2022;145:1124–1138. https://doi.org/10.1093/brain/awab408.
63. Mapplebeck JCS, Beggs S, Salter MW. Molecules in pain and sex: a developing story. *Mol Brain*. 2017;10:9. https://doi.org/10.1186/s13041-017-0289-8.
64. Bretherton B, De Ridder D, Crowther T, Black S, Whelan A, Baranidharan G. Men and women respond equally well to spinal cord and dorsal root ganglion stimulation. *Neuromodulation*. 2022;25:1015–1023. https://doi.org/10.1111/ner.13484.
65. Conic RRZ, Caylor J, Cui CL, et al. Sex-specific differences in the efficacy of traditional low frequency versus high frequency spinal cord stimulation for chronic pain. *Bioelectron Med*. 2022;8:8. https://doi.org/10.1186/s42234-022-00090-2.
66. Mekhail N, Costandi S, Saweris Y, Armanyous S, Chauhan G. Impact of biological sex on the outcomes of spinal cord stimulation in patients with chronic pain. *Pain Pract*. 2022;22:432–439. https://doi.org/10.1111/papr.13097.
67. Yu G, Segel I, Zhang Z, Hogan QH, Pan B. Dorsal root ganglion stimulation alleviates pain-related behaviors in rats with nerve injury and osteoarthritis. *Anesthesiology*. 2020;133:408–425. https://doi.org/10.1097/ALN.0000000000003348.
68. Kramer J, Liem L, Russo M, Smet I, Van Buyten J-P, Huygen F. Lack of body positional effects on paresthesias when stimulating the dorsal root ganglion (DRG) in the treatment of chronic pain. *Neuromodulation*. 2015;18:50–57 [discussion: 57]. https://doi.org/10.1111/ner.12217.
69. Liem L, Russo M, Huygen FJPM, et al. A multicenter, prospective trial to assess the safety and performance of the spinal modulation dorsal root ganglion neurostimulator system in the treatment of chronic pain. *Neuromodulation*. 2013;16:471–482 [discussion: 482]. https://doi.org/10.1111/ner.12072.
70. Mekhail N, Deer TR, Poree L, et al. Cost-effectiveness of dorsal root ganglion stimulation or spinal cord stimulation for complex regional pain syndrome. *Neuromodulation*. 2021;24:708–718. https://doi.org/10.1111/ner.13134.
71. Serra J, Campero M, Ochoa J, Bostock H. Activity-dependent slowing of conduction differentiates functional subtypes of C fibres innervating human skin. *J Physiol*. 1999;515:799–811. https://doi.org/10.1111/j.1469-7793.1999.799ab.x.
72. Weidner C, Schmelz M, Schmidt R, Hansson B, Handwerker HO, Torebjörk HE. Functional attributes discriminating mechano-insensitive and mechano-responsive C nociceptors in human skin. *J Neurosci*. 1999;19:10184–10190. https://doi.org/10.1523/JNEUROSCI.19-22-10184.1999.
73. Thalhammer JG, Raymond SA, Popitz-Bergez FA, Strichartz GR. Modality-dependent modulation of conduction by impulse activity in functionally characterized single cutaneous afferents in the rat. *Somatosens Mot Res*. 1994;11:243–257. https://doi.org/10.3109/08990229409051392.
74. Gee MD, Lynn B, Cotsell B. Activity-dependent slowing of conduction velocity provides a method for identifying different functional classes of c-fibre in the rat saphenous nerve. *Neuroscience*. 1996;73:667–675. https://doi.org/10.1016/0306-4522(96)00070-X.

COMMENTS

This carefully performed electrophysiological study in anesthetized rats demonstrates that DRG stimulation using clinically relevant waveform parameters induces activity in rapidly conducting sensory neurons recorded in their distal processes, supporting the possibility that centrally conducted activity in these units could drive dorsal horn and brainstem analgesic activity. Their observation that the net impulse traffic induced in this neuronal population decreases with time during stimulation, and that such decrease is greater as stimulation frequency increases, together suggest that low frequencies and periodic pauses of stimulation may be beneficial in optimizing this component of DRG stimulation analgesia. Future DRG stimulation studies with behavioral outcomes will be necessary to sort out the comparative roles ofthese large fiber-driven indirect "gate control" and descending modulation mechanisms, vs DRG stimulation-induceddirect blockade of small fiber conduction through the neuronal T-junction. It is quite possible that both play a role, and thattheir relative contributions could be modulated by stimulation parameter designs.

Quinn Hogan, MD
Milwaukee, WI, USA

***

I would like to congratulate the authors on this wonderful manuscript. The manuscript is well written and addresses a very important topic in the neuromodulation field, as our current understanding of DRGS, its modes of action, and optimal stimulation paradigms are still rather limited. Over the last few years, the focus has shifted to use of lower stimulation frequencies and incorporation of microdosing strategies to both maintain (or increase) efficacy, while simultaneously maintaining battery life. The present manuscript adds to this view by describing a series of well conducted experiments to assess the effect of DRGS on recruitment of Aα/Aβ fibers, where lower DRGS frequencies maintain most fiber activation.

Glenn Franken, MSc
Maastricht, The Netherlands

***

The authors present an excellent manuscript studying the mechanisms of action of DRGS. They demonstrate that when applying clinically relevant stimulation parameters, low-frequency (eg, 5 Hz) DRGS, or brief pauses (eg, 2 minutes) in DRGS may promote more consistent activation of large-diameter myelinated sensory neurons. More consistent activation of large-diameter sensory neurons may more effectively engage pain-gating circuits in the spinal cord. This is a great example of a preclinical study that can directly inform the clinical implementation of a neuromodulation therapy.

Robert D. Graham, PhD
Ann Arbor, MI, USA